Heat shock protein B6 potently increases non-small cell lung cancer growth

SHAOMU CHEN, HAITAO HUANG, JIE YAO, LIANGBIN PAN and HAITAO MA

Department of Cardiothoracic Surgery, The First Affiliated Hospital of Soochow University, Suzhou, Jiangsu 215006, P.R. China

Received June 30, 2013; Accepted March 4, 2014

DOI: 10.3892/mmr.2014.2240

Abstract. The aim of the present study was to address the effects of heat shock protein B6 (HspB6) on tumor growth and metastasis in BALB/c mice. Lewis lung carcinoma (LLC) cells were subcutaneously injected into BALB/c mice followed by intraperitoneal injection of recombinant HspB6 (HspB6 groups) or phosphate-buffered saline (control groups). Tumor growth and metastasis were assessed by size measurement and weighing of tumors and cervical lymph nodes, respectively. Chemokine expression in tumor masses was quantified quantitative polymerase chain reaction and western blotting. Tumor cell apoptosis was detected by flow cytometric analysis. The proliferation and migration of LLC cells, stimulated with HspB6, were detected using Cell Counting Kit 8 and wound scratch assays *in vitro*. Tumors grafted into the BALB/c mice and intraperitoneally injected with HspB6 were significantly bigger in size than those grafted into the control mice. From 7 days following the injection, the weight of cervical lymph nodes in HspB6 groups was higher than that in the control mice. We also revealed that the apoptotic cell number in tumor masses in the HspB6 groups was lower than that of the control mice. CD31 expression of vascular endothelial cells was higher in tumors grafted in HspB6 groups than those grafted in the control mice. Concomitantly, the tumor tissue mRNA and protein expression enhancement of vascular endothelial growth factor, basic fibroblast growth factor and intercellular adhesion molecule 1 were greater in HspB6 mice than in the control mice. HspB6 also inhibited cell apoptosis and enhanced the migration and proliferation of LLCs *in vitro*. In conclusion, HspB6 exhibited tumor promotion through increasing tumor angiogenesis, tumor metastasis and inhibiting tumor cell apoptosis.

Correspondence to: Professor Haitao Ma, Department of Cardiothoracic Surgery, The First Affiliated Hospital of Soochow University, 188 Shizi Street, Suzhou, Jiangsu 215006, P.R. China
E-mail: mht7403@163.com

Key words: lung cancer, heat shock protein B6, angiogenesis, metastasis, tumor growth

Introduction

Lung cancer is the most common cause of cancer-related mortality worldwide. With >1,000,000 new cases per year, lung cancer represents the most frequent lethal neoplasm in males, while its incidence increases progressively in females (1). Lung cancer is a heterogeneous disease clinically, histologically, biologically and molecularly (2). The two main types of lung cancer, non-small cell lung cancer (NSCLC; representing 80-85% of cases) and small cell lung cancer (representing 15-20% of cases) are identified based on histological, clinical and immunohistochemical characteristics, and also differ molecularly with numerous genetic alterations exhibiting subtype specificity (3). Despite considerable efforts, only 5-10% of these patients survive 5 years following diagnosis, and surgery accounts for the majority of these long-term survivors (4). Therefore, tumor angiogenesis and tumor metastasis to multiple organs is a critical problem for patients with lung cancer. The prevention and treatment of tumor angiogenesis and tumor metastasis are clinically important (5).

It is well appreciated that heat shock proteins (Hsps) are activated in the mammalian heart in response to numerous physiological or pathological stresses and, consequently, provide cardioprotection (6,7). HspB6, also referred to as Hsp20, belongs to a small Hsp family (15-30 kDa), which includes ≥10 members (HspB1-B10) (8,9). While HspB6 can be detected in various tissues, it is most highly expressed in muscle cells (8-10). Previously, Wang *et al* demonstrated that HspB6-engineered mesenchymal stem cells augmented the secretion of growth factors, including vascular endothelial growth factor (VEGF), basic fibroblast growth factor (bFGF) and intercellular adhesion molecule 1 (ICAM-1), and promoted myocardial angiogenesis (11). Numerous studies indicate that certain Hsps (Hsp90, Hsp70, Hsp60 and aB-crystallin) are detectable outside a variety of cell types, including neuronal cells, monocytes, macrophages, endothelial cells and tumor cells of epithelial origin (12-16). Notably, HspB6 is detectable in the blood and is considered to inhibit platelet aggregation (17). Furthermore, the authors identified what they hypothesized to be a novel function for the extracellular HspB6 in hearts, which was as a mediator of angiogenesis through directly interacting with VEGF receptor 2 (VEGFR-2) (11).

HspB6 is important in endothelial proliferation and tumor growth of several types of cancer (18). However, its effects

on lung cancer and the biological function of HspB6 remain unclear (19,20). To further address the roles of HspB6 in lung cancer, we transplanted Lewis lung carcinoma (LLC) cells into BALB/c mice to examine the roles of HspB6 in the processes of tumorigenesis and metastasis *in vivo*. Tumor size, lymph node weight and angiogenic factors in the tumor growth phase following implantation were detected and compared. In the present study, we provide definitive evidence of the importance of HspB6 in LLC implanted tumor growth and metastasis.

Materials and methods

Reagents and antibodies. Mouse recombinant protein HspB6 was purchased from BioChem Technology, Inc. (Shanghai, China). Alexa Fluor® 488 Annexin V/Dead Cell Apoptosis kit (cat no. V13245) and PE-labeled swine anti-rat IgG polyclonal antibodies were purchased from Invitrogen Life Technologies (Carlsbad, CA, USA). Rat anti-mouse CD31 (MEC13.3) monoclonal antibodies were purchased from BD Pharmingen (San Diego, CA, USA). Goat anti-mouse VEGF (sc-1836) polyclonal antibodies, goat anti-mouse bFGF (C-18) polyclonal antibodies and goat anti-mouse ICAM-1 (sc-1511) polyclonal antibodies were purchased from Santa Cruz Biotechnology, Inc. (Santa Cruz, CA, USA).

Cell line and mice. LLC cells, a murine NSCLC cell line, was purchased from Shanghai Biotechnology (Shanghai, China). Cells were maintained in DMEM (Sigma-Aldrich, St. Louis, MO, USA) supplemented with 10% FCS. BALB/c mice weighing 20-25 g were kindly supplied by the Immunology Laboratory of Soochow University (Suzhou, China) and were kept in our animal facility under specific pathogen-free conditions. All animal experiments were approved by the Guideline for the Care and Use of Laboratory Animals of the Chinese Medical Academy and the Soochow University Animal Care Committee (Suzhou, China). Animals were kept in groups of five and fed regular laboratory chow and water *ad libitum*. A 12-h day and night cycle was maintained.

Cell culture and tumor implantation model. LLC cells were grown in RPMI-1640 culture medium (Invitrogen Life Technologies, Grand Island, NY, USA) containing 10% FBS, 2 mM L-glutamine, 2 mM sodium pyruvate, 20 mM HEPES, 1% non-essential amino acids, 100 μg/ml streptomycin and 100 U/ml penicillin. Cells were maintained at 37˚C with 5% CO_2. Cells were progressively passed to larger plates and allowed to reach ~90% confluence. Cells were harvested by trypsinization, washed with HBSS buffer (Invitrogen Life Technologies) three times and resuspended at a density of $1.0x10^7$ cells/ml in serum-free HBSS buffer. LLC cells ($1x10^6$) in 100 μl HBSS buffer were injected subcutaneously into 8-week-old male BALB/c mice. Tumor growth was assessed on days 6, 8, 10, 14, 16 and 18 after LLC cells injection by the measurement of two bisecting diameters in each tumor using calipers. The size of the tumor was determined by direct measurement of the tumor dimensions. The volume was calculated according to the equation: $V = (LxW^2) \times 0.5$, where V=volume, L=length and W=width (21). On day 14 following tumor implantation, the mice were anesthetized and sacrificed by dislocation of the cervical spine, and the tumor tissues were dissected and weighed.

Table I. Specific sets of primers of qPCR.

Gene	Primer sequences
VEGF	F: 5'-CGCCGCAGGAGACAAACCGAT-3'
	R: 5'-ACCCGTCCATGAGCTCGGCT-3'
bFGF	F: 5'-AAGAGCGACCCACACGTCAAAC-3'
	R: 5'-GTAACACACTTAGAAGCCAGCAGCC-3'
ICAM-1	F: 5'-CCGGTCCTGACCCTGAGCCA-3'
	R: 5'-ATTGGACCTGCGGGGTGGGT-3'
GAPDH	F: 5'-ACCACAGTCCATGCCATCAC-3'
	R: 5'-TCCACCACCCTGTTGCTGTA-3'

qPCR, quantitative polymerase chain reaction; F, forward primer; R, reverse primer; VEGF, vascular endothelial growth factor; bFGF, basic fibroblast growth factor; ICAM-1, intercellular adhesion molecule 1.

Macroscopic assessments of cervical lymph node metastasis. The mice were sacrificed on day 14 following the implantation of LLC cells, and cervical tissues surrounding tumor masses were excised *en bloc*. The nearby cervical lymph nodes were removed and their weights were measured immediately.

Quantitative polymerase chain reaction (qPCR). Total RNA was extracted from LLC cells using an RNeasy Mini kit (Qiagen, Tokyo, Japan). The resultant RNA preparations were further treated with ribonuclease-free deoxyribonuclease (DNase) I (Invitrogen Life Technologies Inc., Gaithersburg, MD, USA) to remove genomic DNA. Total RNA (2 μg) was reverse-transcribed at 42˚C for 1 h in 20 μl of reaction mixture containing mouse Moloney leukemia virus reverse transcriptase and hexanucleotide random primers (Qiagen). The PCR solution contained 2 μl of cDNA, the specific primer set (0.2 μM final concentration) and 12.5 μl of SYBR Premix Ex Taq™ (SYBR Premix Ex Taq Perfect Real-Time PCR kit; Takara, Bio, Inc., Shiga, Japan) in a final volume of 25 μl. qPCR was performed using an iCycler iQ Multicolor Real-Time PCR Detection system (170-8740; Bio-Rad, Hercules, CA, USA). The PCR parameters were as follows: Initial denaturation at 95˚C for 1 min, followed by 40 cycles of 95˚C for 5 sec and 60˚C for 30 sec. The relative gene expression levels were calculated using the $2^{-\Delta\Delta Ct}$ method, where Ct represents the threshold cycle, and GAPDH was used as a reference gene. The primer sequences are shown in Table I.

Western blot analysis. Cell lysates from dissected tumor tissues 14 days following injection were prepared. Briefly, protein samples were dissolved in Laemmli buffer (Bio-Rad), boiled for 5-10 min and centrifuged for 2 min at 10,000 x g to remove insoluble materials. Protein (30 μg per lane) was separated by SDS/PAGE (12%; Bio-Rad) and transferred onto Immobilon-P membranes (Millipore, Bedford, MA, USA). The inhibited membranes were probed overnight (4˚C) with goat anti-mouse VEGF, bFGF or ICAM-1 antibodies (Santa Cruz Biotechnology, Inc.; sc-1836, 1:100), respectively, and rabbit anti-mouse GAPDH (Santa Cruz Biotechnology, Inc.; N-21, 1:200). Subsequently, the membranes were incubated

with secondary horseradish peroxidase-conjugated antibody and immunoreactive bands were visualized using ECL reagent (Pierce Biotechnology, Inc., Rockford, IL, USA). Immunoreactive bands corresponding to target proteins were quantified by Image J analysis (http://rsb.info.nih.gov/ij/download.html) and normalized to those of GAPDH. Blots are representative of at least three experiments.

Flow cytometric analysis of CD31-positive and apoptotic cells. Tumor tissues dissected from BALB/c mice were minced with scissors and were homogenized using a homogenizer in RPMI-1640 medium. Cell suspensions were then passed over a nylon filter with a 100-μm pore size. The resultant cells were further stained with rat anti-mouse CD31 mAb followed by staining with PE-conjugated swine anti-rat IgG mAb. Fluorescence intensities were determined using a FACSCalibur (Becton-Dickinson, Franklin Lakes, NJ, USA), together with the samples stained with non-immunized swine IgG as an isotype control. In the apoptosis assay, cell suspensions were washed in cold phosphate-buffered saline (PBS) in the absence of an inducing agent. The resultant cells were re-centrifuged and the supernatant was discarded. Cell pellets were resuspended in 100 μl/test annexin-binding buffer. Alexa Fluor® 488 annexin V (5 μl; component A) and 1 μl 100 μg/ml of PI working solution were added to each 100-μl cell suspension followed by incubation at room temperature for 15 min. Following the incubation period, 400 μl of 1X annexin-binding buffer was added, gently mixed and kept on ice. As soon as possible, the stained cells were analyzed by a flow cytometry calibur.

Wound scratch assays. In order to explore the effects of HspB6 on the migration of LLC cells, wound scratch assays were performed. The assay was simple and inexpensive and the experimental conditions can be easily modified for different purposes. In brief, cells were seeded into six-well plates at a density that, following 24 h of growth, reached 70-80% confluence as a monolayer. The monolayer was gently, slowly and perpendicularly scratched with a new 1-ml pipette tip across the center of the well. The resulting gap distance was therefore equal to the outer diameter of the end of the tip. Following this, the wells were gently washed twice with medium to remove the detached cells. Subsequently, the wells were replenished with fresh medium. Cells were treated with 1 μg/ml of human recombinant HspB6 in experimental wells and PBS in control wells. Cells were grown for an additional 48 h and images of the cells were captured on a microscope (BX43; Olympus Imaging, Shinjuku, Tokyo, Japan) at 0, 12, 24 and 48 h. The gap distance was quantitatively evaluated using Image J software. Each experimental group was repeated multiple times.

Determination of the rate of cell proliferation. The rate of proliferation was determined using Cell Counting Kit 8 (CCK8; Dojindo Laboratories, Kumamoto, Japan). Cells ($5x10^3$ cells per well) were incubated in 96-well plates and maintained in complete medium 24 h following HspB6 stimulation. After 48, 96 and 120 h, 10 μl of sterile CCK8 dye was added to the cells and incubated for 4 h at 37˚C. Spectrometric absorbance at a wavelength of 450 nm was measured on an enzyme immunoassay analyzer (ELx-800; Molecular Devices, Sunnyvale, CA, USA) following 4 h of incubation. Experiments were performed at least three times, with six replicate measurements, and data are presented as the mean optical density ± standard deviation.

Statistical analysis. The means and standard error of the mean were calculated for all parameters determined in the study. Data were analyzed statistically using one-way analysis of variance or two-tailed Student's t-test. $P<0.05$ was considered to indicate a statistically significant difference.

Results

Tumor growth and angiogenesis is enhanced in HspB6-injected groups. To investigate the effects of HspB6 in tumor growth, we firstly grafted LLC cells subcutaneously into HspB6-injected group and control group mice, and evaluated the development of solid tumors surrounding the injection sites. The tumors in the HspB6-injected groups were significantly larger in size than those in the control groups after day 8. On day 14 following implantation, the mean tumor mass in HspB6-injected groups was increased to almost double of that in the control mice (Fig. 1A and B). Flow cytometry examination of the xenografts revealed that the vascularization of tumor tissues was markedly increased by intraperitoneal injection of HspB6 (Fig. 2A and C). CD31 expression of vascular endothelial cells was ~25% higher in tumors grafted in the HspB6-injected groups than those grafted in the control groups (Fig. 2C).

Tumor metastasis is enhanced in the HspB6-injected groups. To examine the effects of HspB6 in tumor metastasis, cervical lymph nodes surrounding implanted tumor masses were dissected and weighed. We revealed that the weights of the cervical lymph nodes were markedly increased in HspB6-injected groups implanted with LLC cells in comparison with those of the nodes in the control mice. (Fig. 3A). The subcutaneous implantation of LLC cells in HspB6-injected groups was demonstrated to result in enhanced metastatic growth in the cervical lymph nodes combined with promoting the tumor volume at the implanted site.

HspB6 reduces cell apoptosis. To rule out the possibility that the inhibition of cell growth was due to cytotoxic effects, an apoptosis assay was performed. Cells positive for Annexin V-FITC and negative for PI are in the early stage of apoptosis, as shown in the Q4 quadrant, while cells positive for Annexin V-FITC and PI are in the late stages of apoptosis or necrosis, as shown in the Q2 quadrant (22). Thus, the degree of apoptosis correlates with the amount of positive Annexin V-FITC cells. As depicted in Fig. 2B and 2D, there is little binding of Annexin V-FITC on tumor cells implanted in the HspB6 groups compared with the tumor cells implanted in the control mice. The binding for the control mice group ranges from 9.7±2.5 to 12.8±3.1% on day 14. While the binding for the HspB6 group decreased from 6.9±2.7 to 9.5±2.6% on day 14. Combined with these observations, it is clear that the effect of HspB6 on LLC tumors is primarily mediated by reducing apoptotic cell death.

Angiogenic factor gene and protein expression is increased in tumor masses implanted in HspB6 mice. The increased tumor angiogenesis caused large tumor foci in the xenografts

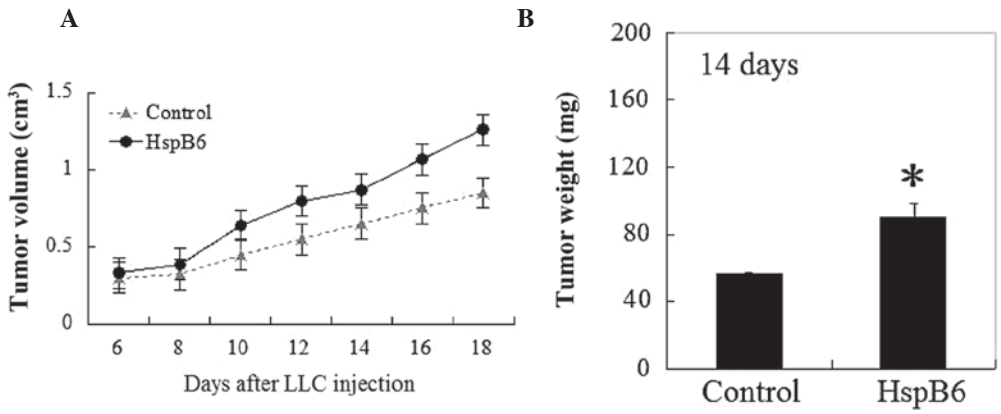

Figure 1. Growth of LLC cells subcutaneously implanted into BALB/c mice. A total of 10^6 cells were injected into the subcutaneous tissue of male BALB/c mice. (A) Tumor volumes were scored on the indicated days as described in Material and methods. (B) On day 14 following implantation, the tumor tissues were dissected and weighed. Results are presented as the means ± SEM. (n=8). LLC, Lewis lung carcinoma; HspB6, heat shock protein B6.

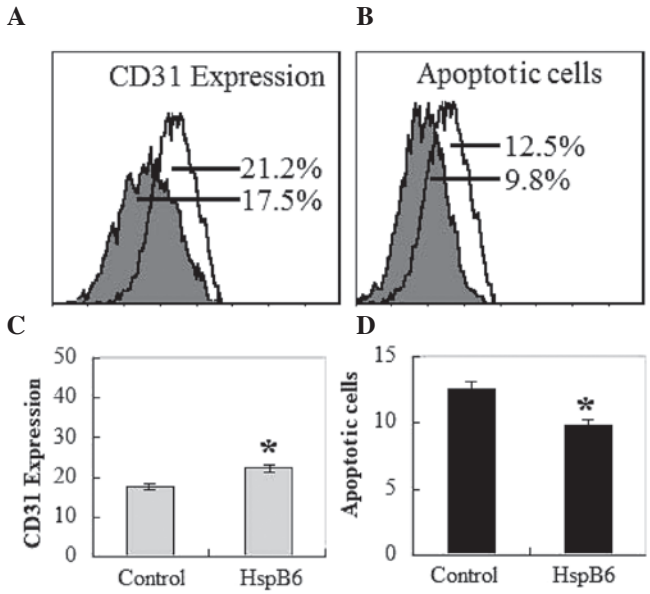

Figure 2. CD31 expression and apoptotic cells in implanted tumor masses analyzed by flow cytometry. On day 14 following implantation, cells were obtained from implanted tumor masses by dissection and homogenization. Flow cytometry analysis of cells stained with (A) CD31 antibodies for the detection of CD31-positive cells or (B) Annexin V and PI for the detection of apoptotic cells. (C) CD31 expression or (D) PI-positive cells were measured from tumor masses in the HspB6 groups and the control mice. There was a significantly higher proportion of CD31 or low PI-positive cells for HspB6 groups, confirming that there was more tumor angiogenesis and less apoptotic cells in LLC implanted tumor masses in the HspB6 groups. LLC, Lewis lung carcinoma; PI, propidium iodide; HspB6, heat shock protein B6.

of HspB6 groups, however not in the control groups. We also identified that the expression levels of VEGF, bFGF and ICAM-1 protein and mRNA in tumor tissues were markedly higher in HspB6 groups than in the control mice (Fig. 4A and B). The increasing result was confirmed by quantification of the relative abundance of VEGF, bFGF and ICAM-1 to GAPDH using a densitometer (Fig. 4A and C). These results suggest that HspB6 is important in tumor-associated VEGF, bFGF and ICAM-1 production and the accompanying angiogenesis.

Migration restoration is induced following wound scratching with HspB6 stimulation. In order to further delineate the effects of HspB6 on the biological function of LLCs, we next examined the roles of HspB6 on the migration of LLC cells. LLCs efficiently seal linear scratch wounds following 48 h of culture, and this migratory process was clearly induced by HspB6 supplemented into the culture medium. Cell migration into the wounded area was markedly increased after 24 h in the HspB6 stimulation group (Fig. 5A). These data indicated that an increase in the migration of LLCs following HspB6 stimulation was responsible for the attenuated wound healing response.

Effects on the proliferation of LLCs. To investigate the biological result of HspB6, we also examined the proliferation of LLCs. With the stimulation of HspB6, the proliferation of LLCs was determined by the MTT assay. HspB6 promotes cell proliferation, as determined by the MTT assay, up to 24 h following stimulation with HspB6 (Fig. 5B).

Discussion

HspB6 is recognized to act intracellularly as a molecular chaperone and confers protection against various hazardous conditions (3,23). Zhang *et al* (18) revealed that extracellular HspB6 physically bound to the VEGF receptor and thereby activated the downstream signaling pathway (Akt and ERK). As a result, myocardial angiogenesis was enhanced in HspB6-overexpressing hearts. Overexpression of HspB6 in the heart not only resists stress-triggered cardiomyocyte death via the intrinsic anti-apoptotic pathways, but also causes increased secretion of HspB6 outside cardiomyocytes, which may function in autocrine or paracine signaling, enhancing the survival of cardiomyocytes and non-cardiomyocytes. Furthermore, the circulating HspB6 has been demonstrated to bind to platelets and inhibit their aggregation (20,24), which may be beneficial for the treatment of ischemic heart disease. This suggests that HspB6 may serve as a novel cardiokine and benefits hearts at multiple levels and that the HspB6 protein may have an advantage over VEGF in promoting myocardial angiogenesis. In the present study, we identified a novel role for HspB6 in facilitating LLC tumor growth by measuring the tumor mass volume *in vivo*. This indicated that implanted tumor growth of LLCs was tightly correlated with the HspB6 protein, suggesting a possible novel biological function of the

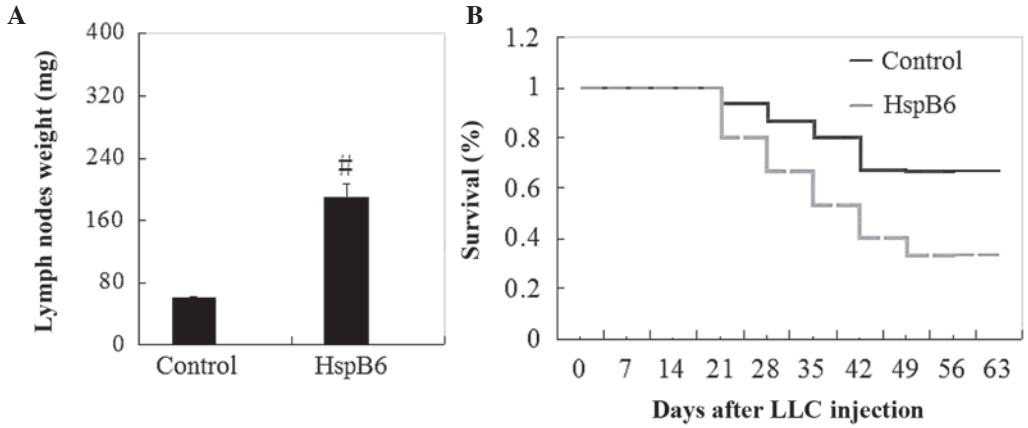

Figure 3. Enhanced tumor metastasis in HspB6 groups. A total of 10^6 cells were subcutaneously injected into male HspB6 groups and control groups of BALB/c mice. On the indicated days following implantation, the mice were sacrificed and the removed cervical lymph surrounding implanted tumor masses were weighed. Results are presented as the means ± SEM (n=10). HspB6, heat shock protein B6; SEM, standard error of the mean.

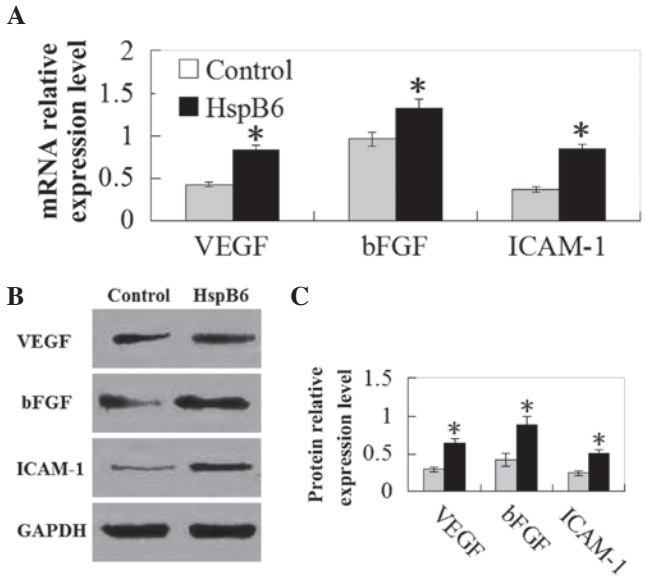

Figure 4. Quantitative polymerase chain reaction and western blot analysis of relative intratumor target gene and protein expression, respectively, in the HspB6 groups and the control mice 14 days following injection of Lewis lung carcinoma cells. (A) mRNA and (B) protein expression ratios of VEGF, bFGF and ICAM-1 to GAPDH in tumor masses of the HspB6 groups and the control groups. (C) Quantification of western blot analysis. Each value represents the mean ± SEM (n=5-8). *P<0.05, compared with the control mice. HspB6, heat shock protein B6; VEGF, vascular endothelial growth factor; bFGF, basic fibroblast growth factor; ICAM-1, intercellular adhesion molecule 1.

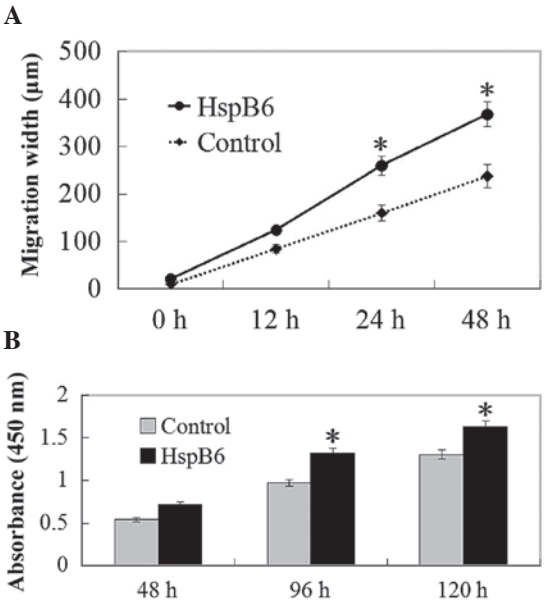

Figure 5. Wound scratch assays and cell proliferation assays to detect the effects of HspB6 on LLC cell migration and proliferation *in vitro*. (A) The LLC cell migration widths were determined. Each value represents the mean ± SEM (n=3). *P<0.05, compared with untreated cells. (B) Optical density values of LLC cell proliferation were determined by ELISA. Each value represents the mean and SEM (n=3). *P<0.05, compared with untreated cells. HspB6, heat shock protein B6; LLC, Lewis lung carcinoma.

HspB6 protein in tumors. This provides a possible therapeutic approach of targeting HspB6 to treat lung cancer.

Lung cancer is notorious for its high probability of lymphatic metastasis even in its early stage. A previous study reported that nodal micrometastases were identified in up to 36% of the resected lungs from the patients with peripheral NSCLC and the presence of metastases to the lymph nodes has been demonstrated to immensely reduce the survival rates (25-27). Consequently, the development of a strategy to suppress lymphatic metastasis appears to be critical in the treatment of lung cancer patients. Among the numerous factors associated with the metastatic process, innate immunity of antitumor metastasis is the first defensive response (28). We hypothesized that HspB6 affects LLC xenografted tumors by inducing tumor cell growth and metastasis. The results of the present study demonstrated that cervical lymph nodes surrounding tumor masses in the HspB6 groups were markedly higher in weight than those in the control mice (Fig. 3). Notably, tumor volumes implanted in HspB6 groups were larger in size compared with those in the control mice (Fig. 1). These findings confirm that HspB6 is crucial in initiating the metastatic process of implanted LLC tumor cells *in vivo* and concomitantly suggesting that they also induce the proliferation of tumor cells.

We also revealed that the mRNA and protein expression of potent angiogenic factors, VEGF, bFGF and ICAM-1, were significantly more enhanced in LLC-implanted tumor tissues in HspB6 groups compared with the control mice. In 1971,

Folkman, who became known as the 'father of tumor angiogenesis', first emphasized the importance of tumor vascularity for tumor growth (29). He described how, if a tumor could be stopped from growing its own blood supply, it would wither and die. Various *in vitro* and *in vivo* studies have since uncovered the role of VEGF as a central player in physiological and pathological angiogenesis (30). Concomitantly, we revealed that LLC implanted tumors exhibited increased angiogenesis in the HspB6 groups more than that in the control mice using anti-mouse CD31 mAb by FACS. These results suggested that HspB6 may be critical in tumor growth by upregulating the expression of VEGF, bFGF and ICAM-1 angiogenic factors and thus increasing tumor angiogenesis. Further exploration regarding the mechanisms by which HspB6 regulates the expression of VEGF, bFGF and ICAM-1 is required. However, the biological function of HspB6 and its regulation of tumor angiogenesis is an interesting topic for clinical discussion.

We also detected the effects of HspB6 on LLC cell migration and cell proliferation *in vitro* by wound scratching and CCK-8 assays, respectively, to observe the direct effects of HspB6 on tumor cells. The results demonstrated that LLC migration and proliferation were induced following HspB6 stimulation. This may provide evidence that HspB6 is critical in tumor growth by multiple pathways, including the promotion of the expression of angiogenic factors, tumor cell migration and tumor cell proliferation. Antagonist-like anti-HspB6 neutralizing antibody could be used to inhibit lung tumor growth.

In summary, we demonstrated that HspB6 is critically involved in LLC implanted tumor growth, tumor metastasis and tumor angiogenesis. The results demonstrated that HspB6 induced tumor growth, tumor metastasis and tumor angiogenesis. Furthermore, the expression of VEGF, bFGF and ICAM-1, the most important of the proangiogenic factors, was enhanced more than in the control mice groups. Furthermore, less apoptotic cells were produced than in the control mice groups. All these findings suggest that HspB6 could enhance cancer growth by the synthesis pathway. Thus, our results provide new information regarding the mechanisms by which HspB6 induces its effects on tumor growth.

Acknowledgements

This study was supported by the Suzhou Natural Science Foundation (no. W2012FZ085).

References

1. Stanley K and Stjernswärd J: Lung cancer - a worldwide health problem. Chest 96: 1S-5S, 1989.
2. Larsen JE and Minna JD: Molecular biology of lung cancer: clinical implications. Clin Chest Med 32: 703-740, 2011.
3. Nakagawa K, Sasaki Y, Kato S, *et al*: 22-Oxa-1alpha, 25-dihydroxyvitamin D3 inhibits metastasis and angiogenesis in lung cancer. Carcinogenesis 26: 1044-1054, 2005.
4. Thatcher N: New perspectives in lung cancer. 4. Haematopoietic growth factors and lung cancer treatment. Thorax 47: 119-126, 1992.
5. Weynants P, Marchandise FX and Sibille Y: Pulmonary perspective: immunology in diagnosis and treatment of lung cancer. Eur Respir J 10: 1703-1719, 1997.
6. Latchman DS: Heat shock proteins and cardiac protection. Cardiovasc Res 51: 637-646, 2001.
7. Willis MS and Patterson C: Hold me tight: Role of the heat shock protein family of chaperones in cardiac disease. Circulation 122: 1740-1751, 2010.
8. Fan GC, Chu G, Kranias EG: Hsp20 and its cardioprotection. Trends Cardiovasc Med 15: 138-141, 2005.
9. Fan GC and Kranias EG: Small heat shock protein 20 (Hsp20) in cardiac hypertrophy and failure. J Mol Cell Cardiol 51: 574-577, 2011.
10. Edwards HV, Cameron RT and Baillie GS: The emerging role of HSP20 as a multifunctional protective agent. Cell Signal 23: 1447-1454, 2011.
11. Wang X, Zhao T, Huang W, *et al*: Hsp20-engineered mesenchymal stem cells are resistant to oxidative stress via enhanced activation of Akt and increased secretion of growth factors. Stem Cells 27: 3021-3031, 2009.
12. Schmitt E, Gehrmann M, Brunet M, *et al*: Intracellular and extracellular functions of heat shock proteins: repercussions in cancer therapy. J Leukoc Biol 81: 15-27, 2007.
13. Calderwood SK, Mambula SS, Gray PJ Jr, *et al*: Extracellular heat shock proteins in cell signaling. FEBS Lett 581: 3689-3694, 2007.
14. Zhan R, Leng X, Liu X, *et al*: Heat shock protein 70 is secreted from endothelial cells by a non-classical pathway involving exosomes. Biochem Biophys Res Commun 387: 229-233, 2009.
15. Song X and Luo Y: The regulatory mechanism of Hsp90alpha secretion from endothelial cells and its role in angiogenesis during wound healing. Biochem Biophys Res Commun 398: 111-117, 2010.
16. Hecker JG and McGarvey M: Heat shock proteins as biomarkers for the rapid detection of brain and spinal cord ischemia: a review and comparison to other methods of detection in thoracic aneurysm repair. Cell Stress Chaperones 16: 119-131, 2011.
17. Niwa M, Kozawa O, Matsuno H, *et al*: Small molecular weight heat shock-related protein, HSP20, exhibits an anti-platelet activity by inhibiting receptor-mediated calcium influx. Life Sci 66: PL7-PL12, 2000.
18. Zhang X, Wang X, Zhu H, *et al*: Hsp20 functions as a novel cardiokine in promoting angiogenesis via activation of VEGFR2. PLoS One 7: e32765, 2012.
19. Noda T, Kumada T, Takai S, *et al*: Expression levels of heat shock protein 20 decrease in parallel with tumor progression in patients with hepatocellular carcinoma. Oncol Rep 17: 1309-1314, 2007.
20. Myung JK, Afjehi-Sadat L, Felizardo-Cabatic M, *et al*: Expressional patterns of chaperones in ten human tumor cell lines. Proteome Sci 2: 8, 2004.
21. Srivastava S, Lundqvist A and Childs RW: Natural killer cell immunotherapy for cancer: a new hope. Cytotherapy 10: 775-783, 2008.
22. Levy EM, Roberti MP and Mordoh J: Natural killer cells in human cancer: from biological functions to clinical applications. J Biomed Biotechnol 2011: 676198, 2011.
23. Hwang YJ, Kim J, Park DS and Hwang KA: Study on the Immunomodulation Effect of Isodon japonicus Extract via Splenocyte Function and NK Anti-Tumor Activity. Int J Mol Sci 13: 4880-4888, 2012.
24. Kozawa O, Matsuno H, Niwa M, *et al*: HSP20, low-molecular-weight heat shock-related protein, acts extracellularly as a regulator of platelet functions: a novel defense mechanism. Life Sci 72: 113-124, 2002.
25. Ichinose Y, Yano T, Asoh H, *et al*: Prognostic factors obtained by a pathologic examination in completely resected non-small-cell lung cancer. An analysis in each pathologic stage. J Thorac Cardiovasc Surg 110: 601-605, 1995.
26. van Velzen E, Snijder RJ, Brutel de la Rivière A, *et al*: Type of lymph node involvement influences survival rates in T1N1M0 non-small cell lung carcinoma. Lymph node involvement by direct extension compared with lobar and hilar node metastases. Chest 110: 1469-1473, 1996.
27. Mountain CF and Dresler CM: Regional lymph node classification for lung cancer staging. Chest 111: 1718-1723, 1997.
28. Costantini C and Cassatella MA: The defensive alliance between neutrophils and NK cells as a novel arm of innate immunity. J Leukoc Biol 89: 221-233, 2011.
29. Folkman J: Tumor angiogenesis: therapeutic implications. N Engl J Med 285: 1182-1186, 1971.
30. Senger DR, Galli SJ, Dvorak AM, *et al*: Tumor cells secrete a vascular permeability factor that promotes accumulation of ascites fluid. Science 219: 983-985, 1983.